molecular systems biology

Targeted interactomics reveals a complex core cell cycle machinery in *Arabidopsis thaliana*

Jelle Van Leene[1,2], Jens Hollunder[1,2], Dominique Eeckhout[1,2], Geert Persiau[1,2], Eveline Van De Slijke[1,2], Hilde Stals[1,2], Gert Van Isterdael[1,2], Aurine Verkest[1,2], Sandy Neirynck[1,2], Yelle Buffel[1,2], Stefanie De Bodt[1,2], Steven Maere[1,2], Kris Laukens[3], Anne Pharazyn[4], Paulo CG Ferreira[5], Nubia Eloy[1,2,5], Charlotte Renne[6], Christian Meyer[6], Jean-Denis Faure[6], Jens Steinbrenner[7], Jim Beynon[7], John C Larkin[8], Yves Van de Peer[1,2], Pierre Hilson[1,2], Martin Kuiper[1,2,10], Lieven De Veylder[1,2], Harry Van Onckelen[4], Dirk Inzé[1,2], Erwin Witters[4,9,11] and Geert De Jaeger[1,2,11,*]

[1] Department of Plant Systems Biology, VIB, Ghent, Belgium, [2] Department of Plant Biotechnology and Genetics, Ghent University, Ghent, Belgium, [3] Department of Mathematics and Computer Science, University of Antwerp, Antwerp, Belgium, [4] Department of Biology, Center for Proteome Analysis and Mass Spectrometry, University of Antwerp, Antwerp, Belgium, [5] Instituto de Bioquímica Médica, Centro de Ciências da Saúde, Universidade Federal do Rio de Janeiro, Rio de Janeiro, Brazil, [6] Institut Jean-Pierre Bourgin, INRA-AgroParisTech, Versailles Cedex, France, [7] School of Life Sciences, Warwick University, Warwick, UK, [8] Department of Biological Sciences, Louisiana State University, Baton Rouge, LA, USA and [9] Flemish Institute for Technological Research (VITO), Mol, Belgium
[10] Present address: Department of Biology, Norwegian University of Science and Technology (NTNU), 7491 Trondheim, Norway
[11] These authors contributed equally to this work
* Corresponding author. Department of Plant Systems Biology, VIB, Ghent University, Technologiepark 927, B-9052 Ghent, Belgium. Tel.: +32 9 3313870; Fax: +32 9 3313809; E-mail: geert.dejaeger@psb.vib-ugent.be

Cell proliferation is the main driving force for plant growth. Although genome sequence analysis revealed a high number of cell cycle genes in plants, little is known about the molecular complexes steering cell division. In a targeted proteomics approach, we mapped the core complex machinery at the heart of the *Arabidopsis thaliana* cell cycle control. Besides a central regulatory network of core complexes, we distinguished a peripheral network that links the core machinery to up- and downstream pathways. Over 100 new candidate cell cycle proteins were predicted and an in-depth biological interpretation demonstrated the hypothesis-generating power of the interaction data. The data set provided a comprehensive view on heterodimeric cyclin-dependent kinase (CDK)–cyclin complexes in plants. For the first time, inhibitory proteins of plant-specific B-type CDKs were discovered and the anaphase-promoting complex was characterized and extended. Important conclusions were that mitotic A- and B-type cyclins form complexes with the plant-specific B-type CDKs and not with CDKA;1, and that D-type cyclins and S-phase-specific A-type cyclins seem to be associated exclusively with CDKA;1. Furthermore, we could show that plants have evolved a combinatorial toolkit consisting of at least 92 different CDK–cyclin complex variants, which strongly underscores the functional diversification among the large family of cyclins and reflects the pivotal role of cell cycle regulation in the developmental plasticity of plants.
Molecular Systems Biology 6:397; published online 10 August 2010; doi:10.1038/msb.2010.53
Subject Categories: plant biology; metabolic & regulatory networks
Keywords: *Arabidopsis thaliana*; cell cycle; interactome; protein complex; protein interactions

Introduction

The basic underlying mechanisms of cell division are conserved among all eukaryotes. However, the *Arabidopsis thaliana* (Arabidopsis) genome contains a collection of cell cycle regulatory genes (Vandepoele *et al*, 2002; Menges *et al*, 2005), which is intriguingly large when compared to other eukaryotes. In five regulatory classes, 71 genes are found in Arabidopsis versus only 15 in yeast and 23 in human (Supplementary Table I). They encode cyclin-dependent kinases (CDKs), of which the substrate specificity is determined by association with various cyclins, whereas series of CDK activators and inhibitors regulate their activity (Inzé and De Veylder, 2006; De Veylder *et al*, 2007). Together with genes encoding the retinoblastoma-related (RBR) protein and members of the E2F/DP family, the genes for CDKs, cyclins, and their regulators were defined as the 'core' cell cycle genes in Arabidopsis (Vandepoele *et al*, 2002; Menges *et al*, 2005). This inventory was augmented with the discovery of genes involved in DNA replication (Shultz *et al*, 2007), and mitotic

checkpoint homologs, including proteins of the anaphase-promoting complex (APC), an E3 ubiquitin ligase, which targets cell cycle proteins for degradation by the 26S proteasome (Capron *et al*, 2003). Microarray analysis demonstrated that many of these genes showed a cell cycle phase-dependent expression profile (Menges *et al*, 2005), whereas genetic studies confirmed their role in cell division (Inzé and De Veylder, 2006; De Veylder *et al*, 2007).

Despite the discovery of numerous cell cycle genes, little is known about the corresponding protein interaction network. Therefore, we applied tandem affinity purification (TAP) approach with the aim to isolate and analyze protein complexes for approximately 100 cell cycle proteins, of which most belong to the cell cycle core list (Supplementary Table II). As we focus on cell division and because plants contain only a minor fraction of dividing cells, we previously developed a TAP approach for complex isolation from Arabidopsis cell suspension cultures (Van Leene *et al*, 2007, 2008). These cell suspension cultures consist of undifferentiated dividing cells and therefore they not only serve as a model for plant meristems, but also are well suited to study protein interactions in the absence of developmental processes, pinpointing the basic cell cycle machinery (Menges *et al*, 2003). Furthermore, they provide an unlimited and cheap supply of proliferating cells that express more than 85% of the predicted core cell cycle genes. The expression of almost all core cell cycle regulators and related genes in cell suspension cultures is in agreement with the observation that most of them do not show strong tissue specificity (Menges *et al*, 2005). This approach allowed us to successfully map a first draft of the basic cell cycle complex machinery of Arabidopsis, providing many new insights into plant cell division.

Results and discussion

Mapping the cell cycle interactome

From the list of cell cycle genes described above, 102 proteins were selected as baits (Supplementary Table III). In addition, six interesting proteins that copurified with the baits were chosen for reverse TAP experiments. Cell cultures were stably transformed with transgenes encoding the tagged proteins under control of a constitutive promoter, as it had been previously shown that constitutive bait expression leads to higher complex recovery as compared to expression with endogenous promoters (Van Leene *et al*, 2007). Despite the use of this constitutive promoter that could induce artificial interactions, we observed that accumulation levels of the fusion proteins depend to a large extent on the nature of the bait and are not always higher than those of the corresponding endogenous protein (Van Leene *et al*, 2007). A plausible explanation is the high level of posttranslational regulation among many essential cell cycle proteins. Moreover, given the high ploidy level (8n) of the Arabidopsis cultures we used, the average transgene copy number per cell might be lower than that of the corresponding endogenous gene. A major advantage of this constitutive promoter was that 95% of the baits were successfully produced as TAP-tagged fusion proteins (Figure 1A). At least two independent purifications were performed for each of the expressed baits on extracts from non-synchronized exponentially growing cells, for a total of 303 purifications. A flow cytometric analysis of the collected cell material showed an equal G1–G2 phase distribution (Van Leene *et al*, 2007), covering all cell cycle phases, meaning that apparently interacting proteins might represent different alternative cell phase-specific complexes. Purified proteins were separated on gel and identified by tandem matrix-assisted laser desorption ionization (MALDI) mass spectrometry (MS). Nonspecific interactors and background proteins were determined through control purifications on wild-type cell culture extracts (mock) or extracts from cultures expressing tagged fusions of heterologous green fluorescent protein (GFP), red fluorescent protein (RFP) or β-glucuronidase (GUS; Supplementary Table IV). All proteins identified in these control experiments were subtracted systematically. Although most false positive interactions are discarded by this approach, some artificial and bait-specific interactions might remain in the data set, for example, interactions occasionally generated during cell lysis. Next, redundancy was filtered out for reciprocal interactions found in both directions, retaining the interaction with the highest MS scores. As such, a final non-redundant data set of 857 interactions among 393 proteins was obtained. As a first proof of the robustness of the data, all six reverse TAP experiments confirmed the original interaction. To further assess the quality of the data set and to evaluate its novelty, we screened for the overlap with protein–protein interactions present in public databases and observed that 82% of the interactions are not yet documented in TAIR (Swarbreck *et al*, 2008), InTact (Kerrien *et al*, 2007), Arabidopsis Reactome (Tsesmetzis *et al*, 2008), AtPID (Cui *et al*, 2008), Reactome (Vastrik *et al*, 2007) and The Bio-Array Resource (BAR) for Arabidopsis Functional Genomics (Geisler-Lee *et al*, 2007), providing a huge amount of new information. In addition, this analysis demonstrates the reliability of the data set because 150 known or predicted interactions were confirmed.

We visualized our data set as a network graph according to the 'spoke' model in which proteins share co-complex membership with their immediate interactors through direct or indirect physical binding (Supplementary Figure 1). Hence, caution is required for the interpretation of the data, in particular because bait–prey interactions identified in TAP experiments might not actually represent direct physical interactions. Additional information on the proteins (e.g. periodicity during the cell cycle, localization) or on the bait–prey relationships (e.g. degree of co-expression, known or new interaction) was integrated into the interactome (Figure 2; see also Supplementary Tables V and VI). Moreover, the entire interactome and all discussed subnetworks can be easily visualized through a Cytoscape (Shannon *et al*, 2003) web start, and the data can be consulted in a matrix pivot table (see Figure 3 for more explanation). All protein interactions have been submitted to the IMEx (http://imex.sf.net) consortium through IntAct (Kerrien *et al*, 2007) with the assigned identifier IM-9598.

Computational quality assessment

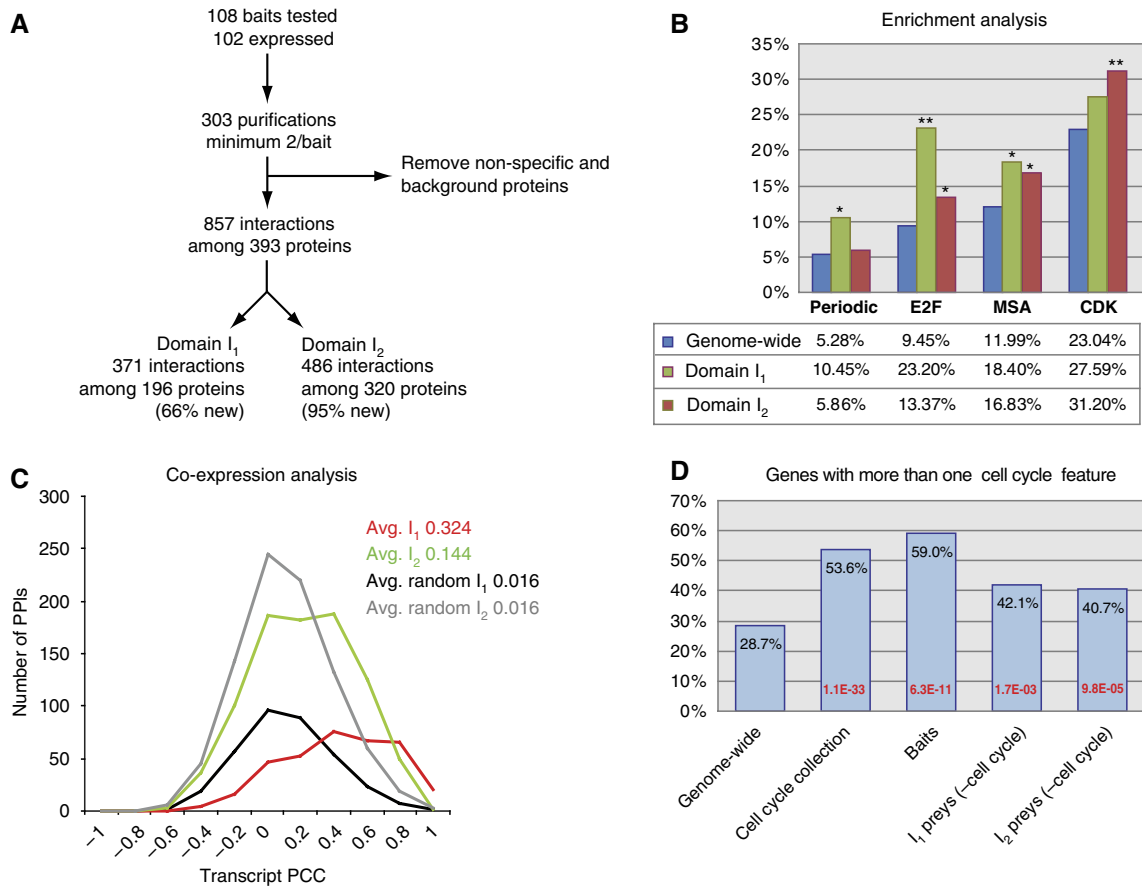To characterize the interactome, we compared two domains that had been identified in the global data set: domain I_1

Figure 1 Generation and computational analysis of the interactome. (**A**) Flow chart of the data generation. (**B**) Enrichment analysis of the data sets for genes showing periodic expression during the cell cycle (Periodic), containing an E2F or MSA promoter motif, and for proteins with a CDK phosphorylation site (CDK). Significance as compared to the genome are indicated with *(P-value <0.05) or with **(P-value <0.01). (**C**) Transcript PCC distributions and average of domain I_1 (red) and I_2 (green), as compared to the average distribution of 100 random corresponding networks (black and gray for I_1 and I_2 data set, respectively). PPI, protein–protein interactions. (**D**) Enrichment analysis for genes with more than one cell cycle feature in different gene sets. The cell cycle gene collection is a list of 518 known cell cycle genes (Supplementary Table IX). The term 'baits' refers to our interactome bait list and '(-cell cycle)' indicates that proteins known to be involved in cell cycle (Supplementary Table IX) were subtracted from domain I_1 and I_2 prey sets. Significance compared to the genome is indicated as P-values in red.

containing 371 interactions confirmed in at least two independent experimental repeats or in the reciprocal purification experiment and domain I_2 consisting of 486 uniquely observed interactions (Figure 1A; Supplementary Figure 1). Several observations underlined the quality of both domains. First, the merged interactions between baits formed a single highly interconnected network (Supplementary Figure 2), reflecting their common involvement in the same biological process. Second, genes encoding preys in domain I_1 and I_2 are enriched for sequences with E2F and M-specific activator (MSA) promoter elements, involved in the G1-to-S and G2-to-M transition, respectively (Figure 1B), thereby demonstrating the successful purification of complexes functioning at S-phase and mitosis. Third, the transcript Pearson Correlation Coefficients (PCCs) that reflect the degree of co-expression correlation were calculated for all interactions, based on an Arabidopsis ATH1 micro-array compendium of experiments focusing on cell cycle or plant growth and development (Supplementary Table VII). On average, a transcript PCC of 0.324 was found for interactions of domain I_1 and 0.144 for domain I_2, which is significantly higher than that of the

average PCC of 100 corresponding random networks (0.016; Figure 1C). These PCCs can be used for confidence assignment to new interactions, because interactors with strong expression correlation are often part of a common molecular assembly (Gunsalus *et al*, 2005). Finally, we identified a large number of new candidate cell cycle genes among the preys of both domains. Therefore, we integrated different cell cycle-related features (Supplementary Table VIII), including periodicity during cell division, CDK phosphorylation sites, and cell cycle-related promoter and protein destruction motifs. In a set of 518 known cell cycle genes (Supplementary Table IX), compiled based on gene ontology (GO) annotation, and supplemented with genes involved in the cell cycle (Vandepoele *et al*, 2002; Capron *et al*, 2003; Menges *et al*, 2005; Shultz *et al*, 2007), a clear enrichment compared to the whole gene pool was detected for genes possessing more than one cell cycle feature (Supplementary Figure 3). The same was true for our bait list, validating the choice of the baits, and for the domain I_1 and I_2 prey lists after subtracting known cell cycle proteins (Figure 1D). Finally, 40 new candidates with more than one feature were extracted from domain I_1 and 83
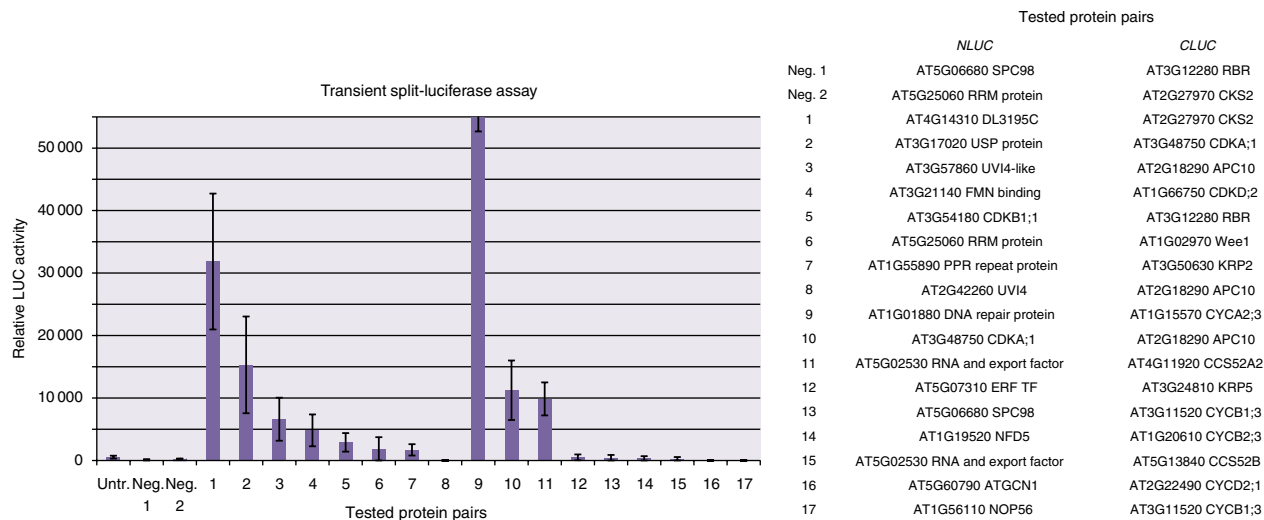
Figure 2 Relative light emission of the different split-luciferase protein pairs. Luciferase (LUC) activity was monitored with at least two independent infiltration experiments per tested interactions (Supplementary Figure 5), except for interactions that could immediately be scored as clearly negative. The mean of the experiments is shown together with the corresponding s.e. values. The mean value of protein pair 9 is shown out of range due to its high value of 70 895. Mean values, s.e. values, the number of replicates and additional information about the protein pairs can be found in Supplementary Table XII. Negative net LUC activity (=Total net LUC activity-background < 0) was set to zero for pairs 8, 16, and 17. All 17 tested pairs are listed next to the graph, together with information regarding which moiety of the luciferase was fused to the protein of interest (NLUC or CLUC). Negative interactions were estimated with two non-interacting TAP protein pairs (Neg.1 and Neg.2). Untr., mean value of untransformed seedlings.

from domain I$_2$ (Supplementary Table X), yielding a total of 106 new candidate cell cycle proteins.

Besides common qualities of both interactome domains, their real significance appeared through mutual differences. For example, 51% of the interactions in domain I$_1$ are between bait proteins, down to only 9% in domain I$_2$. Preys periodically expressed during the cell cycle were enriched solely in domain I$_1$ (Figure 1B), and although both prey sets were enriched for the GO term 'cell cycle', this was not the top hit in domain I$_2$. Here, and in contrast to domain I$_1$, significant enrichment was observed for GO categories related to stress response, phytohormone stimuli, or energy derivation (Supplementary Table XI). A GO similarity analysis (De Bodt *et al*, 2009) between pairs of bait and prey confirmed that, in general, pairs of domain I$_2$ shared only cellular component, a prerequisite for interacting proteins, but not biological process or molecular function, in contrast to pairs of domain I$_1$ (Supplementary Figure 4). These observations reveal two subspaces in the cell cycle interactome: a central regulatory network of stable complexes that are repeatedly isolated and represent core regulatory units, and a peripheral network comprising transient interactions identified less frequently, which are involved in other aspects of the process, such as crosstalk between core complexes or connections with other pathways. Additional evidence for the difference between these two subspaces was obtained when the preys were screened for the presence of CDK consensus phosphorylation sites. An enrichment for preys with CDK phosphorylation motifs was found to be statistically significant only in domain I$_2$ (Figure 1B), but not in domain I$_1$, nor among the uniquely observed interactions of a TAP data set generated with 54 baits unrelated to cell cycle mechanisms (data not shown). Moreover, this observation emphasizes the regulatory role of protein phosphorylation by CDK–cyclin complexes on proteins present in cell cycle-linked pathways.

Biological validation in Arabidopsis plants

As the TAP data set had been generated from complexes purified from cell suspension cultures, we further validated its biological relevance in Arabidopsis plants. For this purpose, we conducted a transient split-luciferase (LUC) assay in cotyledons of Arabidopsis seedlings (Supplementary Figure 5), in which the firefly LUC protein is split into two halves and fused to two different proteins. The firefly LUC activity is only reconstituted when the N- and C-terminal LUC moieties are brought together by the two interacting proteins. This interaction can be visualized with a low-light imaging system (Chen *et al*, 2008). Background signal was defined from untransformed seedlings, for which data were gathered from 27 different experiments providing a mean relative LUC activity of 535 (Untr.). We arbitrary set a relative LUC activity threshold of 4500 for a positive interaction, which is nine-fold higher than that from untransformed seedlings, meaning that values equal or above this threshold is assumed to represent a genuine interaction. A total of 17 new protein pairs were selected for the split-LUC analysis, covering eight interactions from domain I$_1$ and nine from domain I$_2$ (Figure 2; Supplementary Table XII). As negative controls, two protein pairs that did not interact in the TAP data set were tested in the split-LUC assay and these scored negative (Figure 2). Pairs 5, 6, and 7 are considered negative because their relative LUC activity was beneath the threshold, although they might represent true, although weak, interactions because the light signals were significantly higher than those in the negative controls. For both domains together, the success rate was 41% (four positives out of eight tested interactions for domain I$_1$ and three out of nine for domain I$_2$), providing further evidence of the reliability of both data sets. This success rate might be considered high, because the split-LUC assay probes mainly binary interactions and comparative genome-wide analyses

showed that the overlap between binary interaction data and affinity-purified complex data is less than 20% in yeast, demonstrating that different protein interaction techniques detect different subspaces of the total interactome of an organism (Yu *et al*, 2008). Hence, bait–prey interactions discovered by TAP that were negative in this split-LUC assay might represent indirect interactions. Taken together, these validation experiments reveal that both domains contain a

large portion of highly reliable interactions and that the interactions uncovered in cell suspension might well be extrapolated *in planta*.

A bird's eye view on the cell cycle interactome

With respect to insights into the cell cycle physiology, the interactome was subdivided according to the functional
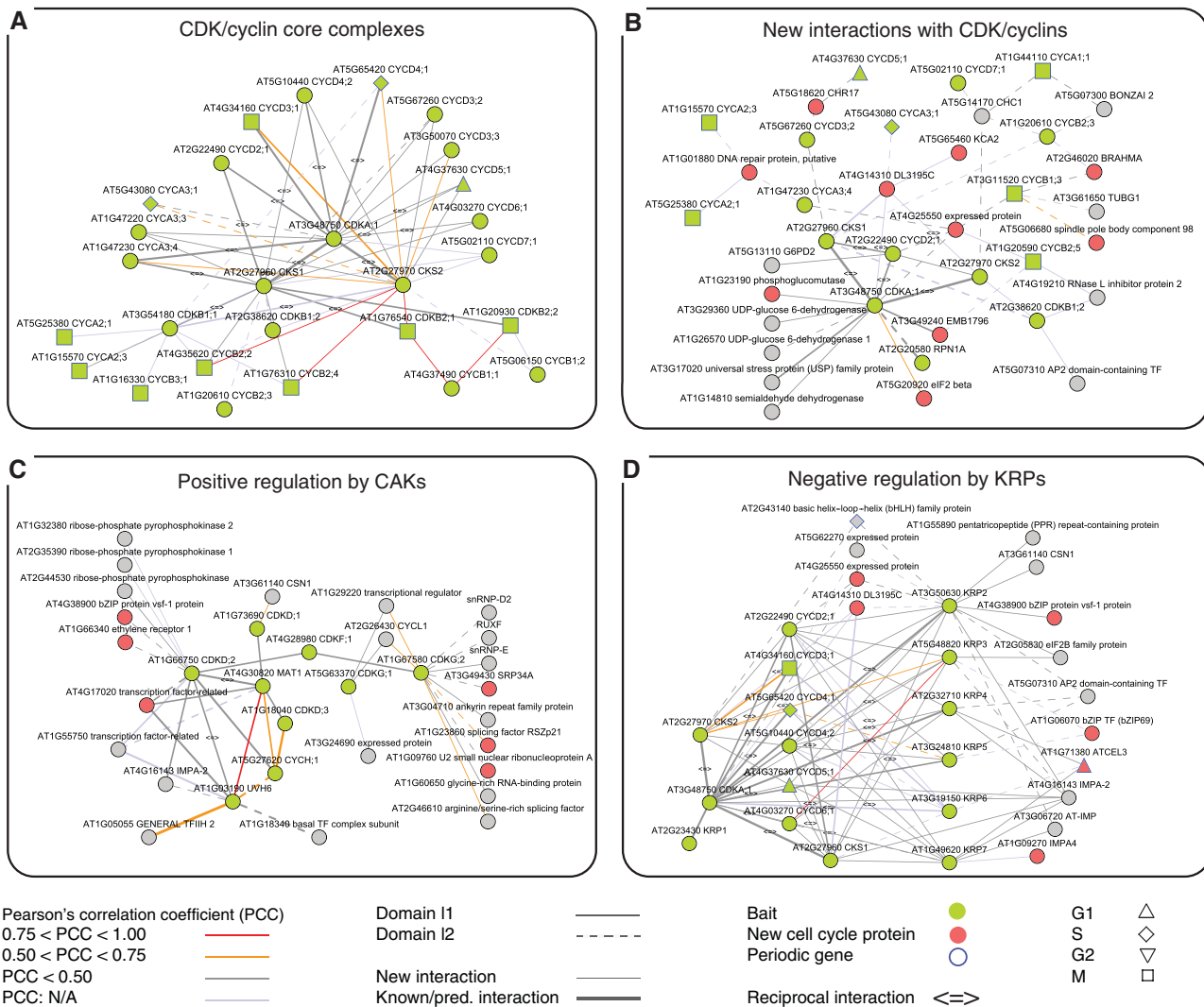

Figure 3 Subnetworks representing the main parts of the interactome. The subnetworks discussed in detail are (**A**) CDK–cyclin core complexes, (**B**) new interactions with CDK–cyclin complexes, (**C**) positive regulation by CAKs, (**D**) negative regulation by KRPs, (**E**) negative regulation by SIM and SIM-related proteins, (**F**) DNA replication complexes, (**G**) the anaphase-promoting complex, and (**H**) spindle checkpoint complexes. The degree of coexpression correlation (PCC) between a gene pair is given as an edge attribute in the color of the edge. Known and predicted interactions were obtained from public databases and can be distinguished from new interactions through the thickness of the edge. Information about which database documented the interaction is provided as an edge attribute in the Cytoscape file in the edge attribute browser. The edge style (solid versus dashed) reflects whether an interactions is confirmed in an experimental repeat or in the reciprocal purification (domain I$_1$) or the interaction was uniquely observed (domain I$_2$). Information about the proteins that were used as bait and about the newly predicted cell cycle proteins is integrated into the color of the nodes. Periodic genes, showing periodicity at transcriptional level during the cell cycle according to a gene list compiled as described in Materials and methods section, are marked with a blue border. The shape of the node refers to the cell cycle phase in which the gene expression peaks according to Menges *et al* (2003). NA, not assessed. The entire interactome and all subnetworks are also available through a Cytoscape web start at http://www.psb.ugent.be/supplementary-data-gejae/512-interactome (username: interactomics, password: CCinteractome). Moreover, the data are presented at this location as an excel pivot table in matrix format allowing easy querying using baits and preys arranged on horizontal and vertical lines, respectively. The filter buttons of the bait allow easy filtering of its preys, and scrolling horizontally gives a clear idea of the specificity of the interaction or crosstalk with other complexes. The numbers in the matrix represent how many times a prey copurified with a given bait. The presence of cell cycle-related features among the preys (Supplementary Table VIII) is also implemented on the horizontal line at the end of the table. Source data is available for this figure at www.nature.com/msb.
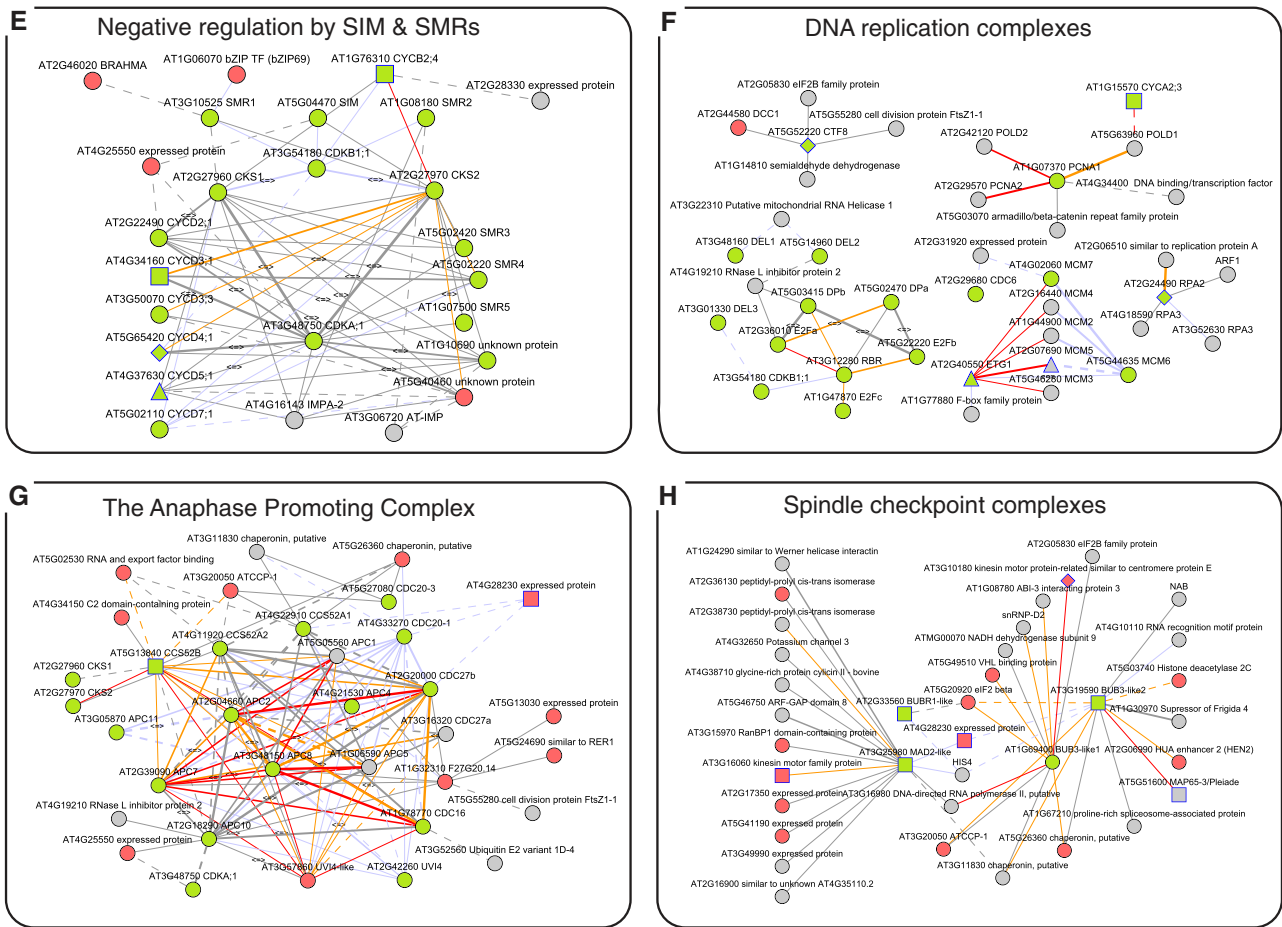
Figure 3 Continued.

classes of the baits (Figure 3) and core protein complexes were derived.

The core CDK–cyclin complexes

From the subnetwork between A- and B-type CDKs and their cyclins (Figure 3A), we extracted CDK–cyclin complexes. CDKA;1, encoded by the constitutively expressed ortholog of yeast *cdc28*, formed stable complexes with constitutively expressed D-type cyclins (e.g. CYCD2;1), with fluctuating D-type cyclins presumed to be active at the cell cycle entry, the G1-to-S transition, or the M-phase (e.g. CYCD3;1), and with S-phase-specific A3-type cyclins (Supplementary Table XIII). On the contrary, A2-type and all B-type cyclins, with an expression peak at the G2-to-M boundary, only bound the plant-specific mitotic B-type CDKs that regulate entry into and progression through mitosis (Menges *et al*, 2005). The B1-type CDKs, peaking earlier than B2-type (Menges *et al*, 2005), bound A2 and B2 cyclins, whereas B2-type CDKs were found exclusively with B1-type cyclins with transcript levels peaking late in M-phase. These results show that our data support transcriptome data (Menges *et al*, 2005) and give a comprehensive overview of A- and B-type CDK–cyclin complexes. Our data imply that mitotic A- and B-type cyclins exclusively form heterodimeric complexes with the plant-specific B-type CDKs

and not with CDKA;1, whereas D-type cyclins associate with CDKA;1. In agreement with the previously described interaction of CDKB2;1 with CYCD4;1 (Kono *et al*, 2003), we observed that CDKB1;1 associated with CYCD4;1; however, as this interaction was found only once, it might reflect a more transient interaction, such as phosphorylation of CDKB1;1 by CDKA;1–CYCD4;1 complexes that regulate its activity. All CDK–cyclin core complexes copurify at least one of the two scaffold CDK subunit (CKS) proteins.

Additional interesting new interactions were identified with core CDKs and cyclins (Figure 3B). A protein of unknown function, AT4G14310, copurified with CDKA;1, CKS1, CKS2, CYCA3;1, CYCA3;4, and KRP2. Reverse purification confirmed interaction with CDKA;1 and CKS2, and revealed interaction with the plant-specific kinesin motor protein KCA2. As the latter is involved in division plane determination (Vanstraelen *et al*, 2006), AT4G14310 might be involved in the same pathway, as supported by the observation that a GFP fusion of AT4G14310 localized at the pre-prophase band (data not shown). Furthermore, CDKA;1 copurified with RPN1a, a regulatory subunit of the 26S proteasome complex, possibly reflecting cell cycle regulation of the 26S proteasome. In addition, 19 proteasome-related proteins were pulled down with this RPN1a subunit of the 26S proteasome. Further, CDKA;1 interacted with three proteins (one phosphoglucomutase and two UDP-glucose 6-

dehydrogenases) from the UDP-xylose biosynthesis pathway, coupling cell cycle regulation with cell wall synthesis (Seifert, 2004). The spindle pole body component 98 and γ-tubulin, two proteins involved in microtubule (MT) nucleation, were pulled down with CYCB1;3. These proteins colocalize at nuclear membranes during G2-phase and are involved in the assembly of pre-prophase band, a plant-specific structure required for polarity determination during cell cycle (Erhardt *et al*, 2002). The interaction with CYCB1;3 appears to be justified because activation of MT nucleation sites and coordinated regulation of the MT assembly might be controlled by cell cycle and/or developmental signals.

Positive regulation of CDK–cyclin complexes

We mapped complexes of CDK-activating kinases (CAKs) that activate CDKs through phosphorylation of a threonine residue in their T-loop. Arabidopsis encodes four CAKs, namely three D-type CDKs and one CAK-activating kinase CDKF;1. Both CDKD;2 and CDKD;3 copurify with CYCH;1 and the CAK assembly factor MAT1 (Figure 3C), which indicates the presence of trimeric CDKD–CYCH–MAT1 complexes in plants, similar to the mammalian D-type CDKs (Devault *et al*, 1995). As in rice (*Oryza sativa*; Rohila *et al*, 2006), CDKD;2 is also part of the basal TFIIH complex involved in transcription and DNA repair, of which three members (UVH6/XPD, AT1G55750 and AT4G17020) copurified. In this complex, CDKD;2 activates transcription through phosphorylation of the C-terminal domain (CTD) of RNA polymerase II. With UVH6 and MAT1 as baits, we confirmed interaction with CDKD;2 and extended the TFIIH complex with two additional proteins (general TFIIH2 and AT1G18340). In addition, the interaction of CDKD;2 with three ribose-phosphate pyrophosphokinases involved in nucleotide biosynthesis, further demonstrated the role of D-type CDKs in the S-phase. Besides the extraction of complexes previously shown in other organisms, our data also suggested new functional links. For example, CDKF;1 does not only interact with its known target CDKD;2 (Shimotohno *et al*, 2004), but also with CDKG;2 (Figure 3C). The G-type CDK class has two members in Arabidopsis and is homologous to the human p58 galactosyltransferase protein associated with cytokinesis (Menges *et al*, 2005). A cyclin with no clear function in the cell cycle, CYCL1, copurified with both CDKGs, validating the clustering of CYCL1 with CDKG;2 in a tissue-specific gene expression analysis (Menges *et al*, 2005). The other proteins forming complexes with CDKG (Figure 3C) and the SR-like splicing domain of CYCL1 (Forment *et al*, 2002) hint at a function in transcription and transcript processing. On the basis of the peak of CDKG transcription (Menges *et al*, 2005), CDKG–CYCL complexes are presumably active at the cell cycle onset.

Negative regulation of CDK–cyclin complexes

Plants not only contain CDK activators but also many negative regulators (Supplementary Table I and II), such as the seven Kip-related proteins (KRPs) in Arabidopsis. The proteins KRP2–KRP7 copurified solely with CDKA;1 and D-type cyclins, suggesting that KRPs only inhibit CYCD–CDKA;1 complexes

(Figure 3D). In addition, KRPs have been postulated to regulate the nuclear import of cell cycle regulators (Zhou *et al*, 2006). Their association with transcription factors suggests that their role in reallocation is not solely targeted to CDK–cyclin complexes (Figure 3D). Another family of cell cycle inhibitors, upregulated by biotic and abiotic stress, comprise SIAMESE (SIM) and SIAMESE-related (SMR) proteins (Churchman *et al*, 2006; Peres *et al*, 2007). Thus far, this family consisted of six proteins (SIM and SMR1–SMR5), but a recent analysis has extended this family with eight additional members (J Van Leene *et al.*, unpublished data; Supplementary Tables I and II). Endoreduplication in trichomes is promoted by SIM by the suppression of mitosis, possibly through inhibition of CDKA;1–CYCD complexes (Churchman *et al*, 2006). However, in our analysis, CDKB1;1, and not CDKA;1 copurified with SIM as bait (Figure 3E), suggesting that endoreduplication might be triggered directly by inhibition of mitotic CDKB complexes. In addition, SMR1 and SMR2 associate with CDKB1;1, and its interactor CYCB2;4 binds AT2G28330 (SMR11), one of the additional members of the SMR family. Until now, such potential inhibitors of B-type CDKs had not been found in plants. In contrast, SMR3–SMR5 and two new members of the SMR clan, AT5G40460 (SMR6) and AT1G10690 (SMR8), clearly associate with CDKA;1 and D-type cyclins. The latter was confirmed by reverse purifications. As SMR6 was induced almost 20-fold in plants co-over-expressing E2Fa and DPa (Vandepoele *et al*, 2005), it might inhibit CDKA;1–CYCD complexes during S-phase, preventing the re-initiation of DNA replication. Similar to KRPs, we also observed nuclear import proteins and transcription factor-related proteins with the SMRs.

Progression to DNA replication and through mitosis

At the G1-to-S boundary, CDK–cyclin complexes activate the E2F–DP pathway by phosphorylation of the repressor RBR, inducing genes involved in nucleotide synthesis, DNA replication, and DNA repair. We confirm that E2Fa and E2Fb associate both with DPa and DPb, and that all E2Fs, including E2Fc, and DP proteins interact with RBR (Figure 3F). Intriguingly, the mitotic CDKB1;1, and not CDKA;1, copurified with RBR, providing additional evidence that the E2F–DP–RBR network is not only active at G1-to-S, but also at G2-to-M transition, as previously suggested for plants (Magyar *et al*, 2005), *Drosophila* (Neufeld *et al*, 1998), and mammalian cells (Ishida *et al*, 2001). Furthermore, because CDKB1;1 interacted with DEL3, an atypical E2F factor lacking the *trans*-activating domain (Lammens *et al*, 2009), we propose that activity of DEL3 might be regulated by CDKB1;1 at the G2-to-M transition, consistent with the observation that both genes are transcribed at that time point and that the encoded proteins can indeed meet each other (Menges *et al*, 2005). Additional complexes involved in DNA replication or repair were isolated (Figure 3F), such as the minichromosome maintenance (MCM) complex, a complex containing the proliferating cell nuclear antigen 1 (PCNA1), which is a sliding clamp for DNA polymerase, the alternative Ctf18 replication factor C complex required for sister chromatid cohesion in yeast (Mayer *et al*,

2001), and a complex involved in stabilization of single-stranded DNA during replication, repair and transcription, including RPA2, two RPA3 proteins, and a putative replication protein (AT2G06510; Shultz *et al*, 2007). The MCM and PCNA complexes are clearly enriched for genes with an E2F motif in their promoter (Supplementary Figure 6), meaning that these complexes are synthesized and assembled just in time at the beginning of S-phase through the E2F–DP pathway. The presence of E2F motifs in the promoters of E2Fb and DPa or E2Fc and RBR reflects positive or negative feedback mechanisms regulating this pathway, respectively (Vandepoele *et al*, 2005).

From the G2-to-M transition onward, unidirectional progression through the cell cycle is, next through the action of CDK–cyclin complexes, further achieved by the APC complex that targets cell cycle proteins for destruction by the 26S proteasome (De Veylder *et al*, 2007). For the first time, a plant APC has been isolated biochemically, and the complex is visualized as a very tightly interconnected network enriched for highly co-expressed gene pairs (Figure 3G). All putative plant APC subunits were identified, except the two small proteins (<10 kDa) APC13 (Bonsai) and Cdc26. However, these proteins were shown not to be essential for proper APC functioning in yeast (Thornton and Toczyski, 2006) and therefore might not belong to the active core complex in plants. We further demonstrate that both Cdc27a and Cdc27b (HOBBIT) can be part of the APC. Three new plant-specific APC interactors (AT1G32310, UVI4, and UVI4-like) were identified and their interaction with the APC was confirmed by reverse purification. The interactor UVI4 has been postulated to keep cells in the mitotic state because mutants for UVI4 showed increased endoreduplication (Hase *et al*, 2006). It is intriguing that this function can be linked now with the APC. A closer look at the protein sequence of UVI4 and UVI4-like revealed different CDK consensus phosphorylation motifs in their sequences, possibly important in the regulation of their activity. Interestingly, both proteins have a C-terminal methionine–arginine (MR) tail. This MR tail is present in only 40 Arabidopsis proteins, whereas in *Xenopus* it is implicated in cdc20-independent binding of Nek2a to the APC (Hayes *et al*, 2006) and resembles the known isoleucine–arginine tail present in the APC activators, involved in binding of the APC activators to the tetratricopeptide repeat-containing APC subunits (Vodermaier *et al*, 2003). Regulation of APC activity could be achieved by CDKA;1, as derived from its interaction with APC10. Analogous to yeast, APC activators in plants are most probably guided to the APC by the action of the CCT chaperonin (Camasses *et al*, 2003), because three such family members copurified.

This chaperonin could also assist in the assembly of other spindle checkpoint complexes, as shown for three Arabidopsis homologs of the mitotic checkpoint proteins Mad2 and Bub3 (Capron *et al*, 2003; Menges *et al*, 2005; Figure 3H). Unattached kinetochores trigger the formation of Mad2–Bub3–BubR1 complex that, in turn, inhibits Cdc20 APC activators, thereby preventing degradation of several cell cycle regulators and progression of anaphase (Kimbara *et al*, 2004). The mitotic checkpoint proteins pulled down many specific interactors, including M-phase-specific kinesins; the highly co-expressed MAP65-3, located at mitotic microtubule arrays and

essential for cytokinesis (Müller *et al*, 2004); histone H4; two peptidyl-prolyl *cis-trans* isomerases; two proteins of the prefoldin chaperone; a helicase (AT1G24290) similar to the replication factor C protein; and an ADP-ribosylation factor GTPase-activating protein (AT3G15970). The latter two proteins had previously been predicted to interact with MAD2-like (Geisler-Lee *et al*, 2007).

The extraction of the subnetwork of genes with an MSA motif in their promoter revealed two small clusters (Supplementary Figure 7), representing a module of the APC connected to a module of a mitotic checkpoint complex by an unknown protein (AT4G28230). Interestingly, DPa and E2Fb possess an MSA motif, supporting our previous hypothesis that the E2F–DP–RB pathway is also active at the G2-to-M transition.

An integrative view on CDK–cyclin complexes

It has been shown that transcriptional diversification during cell cycle progression is a key element among cyclins and core cell cycle regulators in plant cells (Menges *et al*, 2005). We ranked each cyclin along the cell cycle phases according to their peak during transcription and grouped them with their associated CDKs, CKS scaffolding proteins, and negative regulators (Figure 4; Supplementary Table XIII). Modules of interacting proteins were obtained showing an assorted set of CDK–cyclin complexes with high regulatory differentiation. Even within the same subfamily (e.g. cyclin A3, B1, B2, D3, and D4), cyclins differ not only in their functional time frame but also in the type and number of CDKs, inhibitors and scaffolding proteins they bind, further indicating their functional diversification. According to our interaction data, at least 92 different variants of CDK–cyclin complexes are found in Arabidopsis. We speculate that further complex analysis in synchronized cultures will demonstrate an even higher variety. In conclusion, these results reflect how several rounds of gene duplication (Sterck *et al*, 2007) allowed the evolution of a large set of cyclin paralogs and a myriad of regulators, resulting in a significant jump in the complexity of the cell cycle machinery that could accommodate unique plant-specific features, such as an indeterminate mode of post-embryonic development. Through their extensive regulation and connection with multiple up- and downstream pathways, the core cell cycle complexes might offer the sessile plant a flexible toolkit to fine-tune cell proliferation in response to an ever-changing environment.
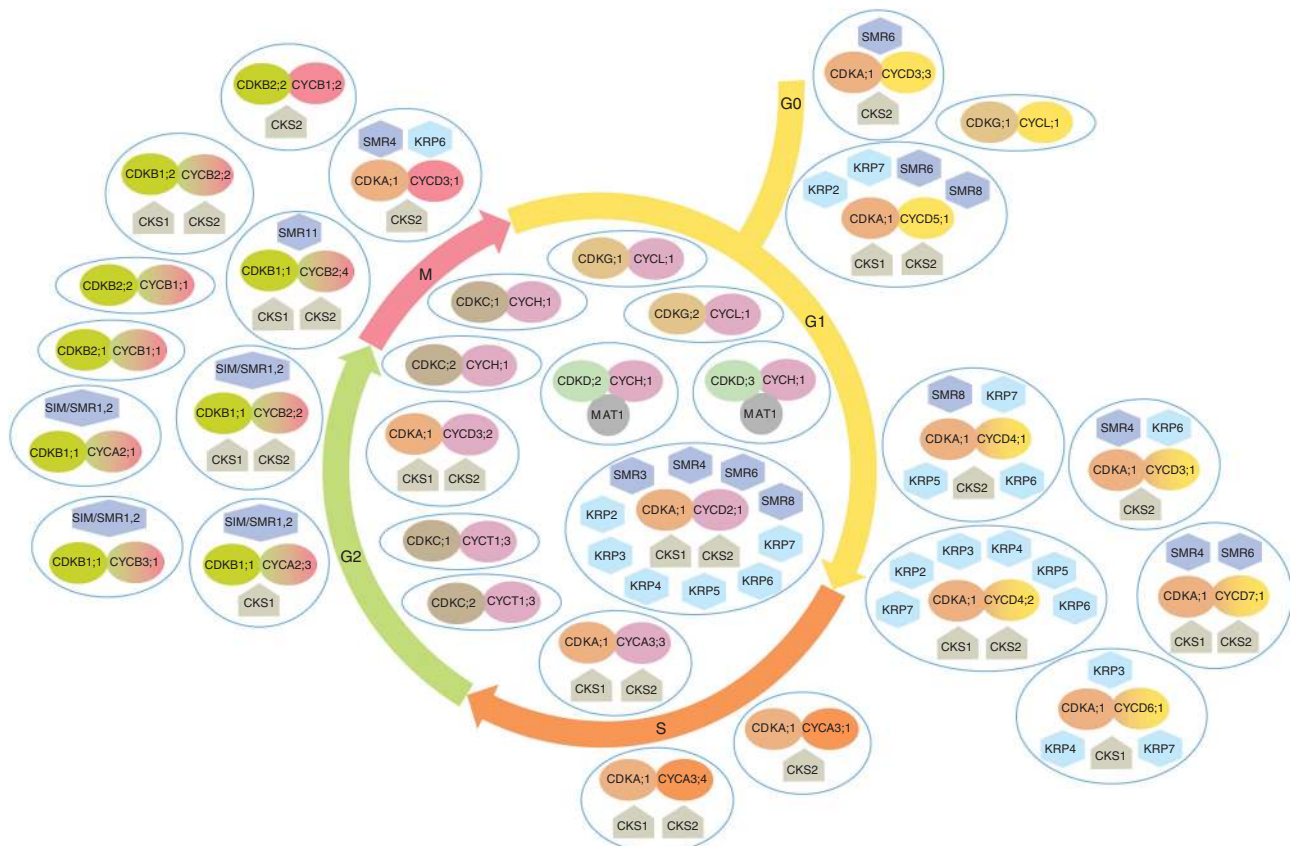
Materials and methods

Figure 4 CDK–cyclin modules extracted from the interactome. Modules were ranked along the cell cycle phases according to the transcript peak level of the cyclin (Supplementary Table XIII). A module consists of a CDK–cyclin complex in the middle, surrounded by its 'core' interactors: CKS docking factors (gray), KRP inhibitors (light blue), or SIM/SMR inhibitors (dark blue). The color of the cyclin corresponds to the cell cycle phase at which its transcript level peaks. For the modules inside the circle, a constant expression profile for the cyclin is observed.

Mass spectrometry

Proteolysis and peptide isolation

After destaining, gel slabs were washed for 1 h in H_2O, polypeptide disulfide bridges were reduced for 40 min in 25 ml of 6.66 mM DTT in 50 mM NH_4HCO_3 and the thiol groups were alkylated sequentially for 30 min in 25 ml of 55 mM iodacetamide in 50 mM NH_4HCO_3. After washing the gel slabs three times with water, complete lanes from the protein gels were cut into slices, collected in microtiter plates, and treated essentially as described before with minor modifications (Van Leene *et al*, 2007). In each microtiter plate well, dehydrated gel particles were rehydrated in 20 µl digest buffer containing 250 ng trypsin (MS Gold; Promega, Madison, WI), 50 mM NH_4HCO_3, and 10% CH_3CN (v/v) for 30 min at 4°C. After adding 10 µl of a buffer containing 50 mM NH_4HCO_3 and 10% CH_3CN (v/v), proteins were digested at 37°C for 3 h. The resulting peptides were concentrated and desalted with microcolumn solid phase tips (PerfectPureTM C18 tip, 200 nl bed volume; Eppendorf, Hamburg, Germany) and eluted directly onto a MALDI target plate (Opti-TOFTM384 Well Insert; Applied Biosystems, Foster City, CA) using 1.2 µl of 50% CH_3CN: 0.1% CF_3COOH solution saturated with α-cyano-4-hydroxycinnamic acid and spiked with 20 fmole/µl glu1-fibrinopeptide B (Sigma Aldrich), 20 fmole/µl des-Pro2-Bradykinin (Sigma Aldrich), and 20 fmole/µl Adrenocorticotropic Hormone Fragment 18–39 human (Sigma Aldrich).

Acquisition of mass spectra

A MALDI tandem MS instrument (4700 and 4800 Proteomics Analyzer; Applied Biosystems) was used to acquire peptide mass fingerprints and subsequent 1-kV CID fragmentation spectra of selected peptides.

Peptide mass spectra and peptide sequence spectra were obtained using the settings essentially as previously presented (Van Leene *et al*, 2007; Supplementary MS data). Each MALDI plate was calibrated according to the manufacturers' specifications. All peptide mass fingerprinting (PMF) spectra were internally calibrated with three internal standards at m/z 963.516 (des-Pro2-Bradykinin), m/z 1570.677 (glu1-fibrinopeptide B), and m/z 2465.198 (Adrenocorticotropic Hormone Fragment 18–39), resulting in an average mass accuracy of 5 ± 10 p.p.m. for each analyzed peptide spot on the analyzed MALDI targets. Using the individual PMF spectra, up to 16 peptides, exceeding a signal-to-noise ratio of 20, which passed through a mass exclusion filter, were submitted to fragmentation analysis.

MS-based protein homology identification

Data search files were generated with the search engine settings presented previously (Van Leene *et al*, 2007; Supplementary MS data) and submitted for protein homology identification against the TAIR 8.0 database (Swarbreck *et al*, 2008) by using a local database search engine (Mascot 2.1, Matrix Science). Protein homology identifications of top hits (first rank) with a relative score exceeding 95% probability were retained. Additional positive identifications (second rank and more) were retained when the score exceeded the 98% probability threshold. Preferentially, identifications resulting from combined searches, PMF, and MS/MS were retained. In addition, PMF-only identifications were retained, but an additional restriction was implemented here. To reduce the number of false positive identifications, PMF-only identifications, for which 50% or more of the matched peptides had a trypsin miscleavage, were discarded.

Data analysis

Enrichment analyses

For the periodic gene identification and enrichment analysis, a list of 1258 genes showing cell cycle-regulated and cell cycle-associated expression was compiled from two data sets (Menges *et al*, 2003; Jensen *et al*, 2006). Genome wide corresponds to all 23 834 genes present on the Affymetrix ATH1 microarray.

Analysis of overrepresentation of GO terms was done using the BiNGO tool (Maere *et al*, 2005) in Cytoscape (Shannon *et al*, 2003). The hypergeometric test was chosen at a significance value of 0.05 with the Benjamini and Hochberg false discovery rate correction for multiple testing (Benjamini and Yekutieli, 2001). The Arabidopsis gene annotation file used in the analysis was downloaded from the GO website on the October 4, 2008.

Genes containing E2F or MSA motifs in their promoter sequence were *in silico* determined by combining transcript expression data and comparative genomics (Vandepoele *et al*, 2006). Here, genome wide corresponds to 19 173 genes for which a unique probe set is available on the ATH1 microarray.

Proteins containing the CDK consensus phosphorylation site [ST]PX[KR], a known hallmark of CDK substrates (De Veylder *et al*, 1997), were considered as potential CDK substrates. The presence of the consensus motif was screened with the patmatch tool available at TAIR (Swarbreck *et al*, 2008), and hence, genome wide corresponds here to all 27 235 proteins present in the TAIR8.0 release.

All enrichment analyses were compared to the genome-wide situation and *P*-values were calculated using a hypergeometric cumulative distribution function. Proteins that could not be assigned to a specific gene locus were discarded from all enrichment analyses.

GO similarity analysis

To calculate the GO similarity scores, GO terms were extracted from the GO database (Ashburner *et al*, 2000) and annotations for Arabidopsis proteins were downloaded from TAIR (Swarbreck *et al*, 2008). For each protein pair, all GO terms of both proteins were compared to each other and GO similarity scores were calculated as described previously (De Bodt *et al*, 2009). For each pair of GO terms, the depth of the common ancestor of the terms, which is the shortest path of the common ancestor to the root (GO:0003673), is calculated. Subsequently, the maximum value of the calculated depths is taken as the GO similarity score for a certain protein pair. The assignment of GO terms based on physical interactions (IPI) or electronically assigned and less reliably assigned GO terms (with evidence codes ND, NR, NAS, and IEA) were removed. In addition, GO similarity scores were calculated for gene pairs from 1000 randomized data sets. For the comparison original versus random network, we considered the subnetwork of the protein interaction network in which each protein–protein interaction could be overlaid with at least one GO term. On the basis of this original subnetwork, we generated 1000 random networks maintaining the number of nodes and interactions containing at least one GO term between the nodes. The nodes were randomly selected from a pool containing all Arabidopsis proteins with at least one GO term. The networks of the three GO categories: biological process, molecular function, and cellular component were analyzed.

Co-expression analysis

Transcript PCCs reflecting the degree of co-expression correlation were calculated on the basis of an Arabidopsis ATH1 microarray compendium of 518 experiments focused toward plant growth and development (Supplementary Table VII). We compared the PCC distribution of both data sets with the PCC distribution of 100 randomized data sets. Similar to the GO similarity analysis, we considered a subnetwork of our protein interaction network containing those interactions that could be addressed with an expression value based on our compendium. The nodes of the random networks were randomly selected from a pool of all Arabidopsis proteins, whereas the number of expression links was maintained.

New candidate cell cycle proteins

Periodic genes, genes with E2Fa-like or MSA-like motifs in the promoter sequence and proteins containing a CDK consensus motif were determined as described above (enrichment analyses). All genes containing the remainder cell cycle-related promoter motifs were determined by the same *in silico* analysis combining transcript expression data and comparative genomics (Vandepoele *et al*, 2006). Proteins containing a PEST motif were determined using the epestfind tool provided by EMBOSS (Rice *et al*, 2000). The D-box corresponds to the amino-acid motif RxxLxxxxN where x is any amino acid, whereas the A-box corresponds to the amino-acid motif QRVL. The GxEN-box corresponds to the amino-acid motif GxEN where x is any amino acid, whereas the KEN-box corresponds to the amino-acid motif KEN. All enrichment analyses were compared to the genome-wide situation and *P*-values were calculated using a hypergeometric cumulative distribution. Proteins that could not be assigned to a specific gene locus were discarded from all enrichment analyses.

Generation of the network in Cytoscape

The cytoscape file, which is accessible through a Cytoscape webstart, was generated in Cytoscape 2.5.1. by importing node and edge attribute files (Supplementary Tables V and VI) representing information regarding proteins and interactions, respectively.

Transient split-luciferase analysis

Firefly luciferase split constructs were generated as described previously (Chen *et al*, 2008). Sequences coding for the N- or C-terminal luciferase moieties were cloned in Gateway pPZP200-based vectors (Karimi *et al*, 2007), either 5′ (for N-terminal fusions of luciferase) or 3′ (C-terminal fusions) to the gateway recombination sequence. This way, we obtained four different vector combinations, allowing insertion of the gene of interest through gateway recombination cloning. Transient transformation was carried out on 15–20 seedlings of Landsberg *erecta* Arabidopsis seedlings grown in six-well plates as described previously (Marion *et al*, 2008). Transformed seedlings were sprayed twice with a 5 mM luciferine solution (synchem OHG) containing 0.01 % Triton X-100 and imaged with an ultra-amplified CCD camera (Photonic Science). Levels of light emissions were obtained after integrating 2000 images (Photolite 32 software). Light signals were quantified within a region of interest corresponding to the entire well and background was subtracted to obtain net light emission. Finally, luciferase emission was normalized according to the number of infiltrated plants estimated by their autofluorescence values. Leaf autofluorescence was measured with an excitation at 635 nm and a long pass filter + 665 nm (FLA5000, FUJI).

Supplementary information

Supplementary information is available at the *Molecular Systems Biology* website (http://www.nature.com/msb).

Conflict of interest

The authors declare that they have no conflict of interest.

References

Ashburner M, Ball CA, Blake JA, Botstein D, Butler H, Cherry JM, Davis AP, Dolinski K, Dwight SS, Eppig JT, Harris MA, Hill DP, Issel-Tarver L, Kasarskis A, Lewis S, Matese JC, Richardson JE, Ringwald M, Rubin GM, Sherlock G (2000) Gene ontology: tool for the unification of biology. *Nat Genet* **25:** 25–29

Benjamini Y, Yekutieli D (2001) The control of the false discovery rate in multiple testing under dependency. *Ann Statist* **29:** 1165–1188

Bürckstümmer T, Bennett KL, Preradovic A, Schütze G, Hantschel O, Superti-Furga G, Bauch A (2006) An efficient tandem affinity purification procedure for interaction proteomics in mammalian cells. *Nat Methods* **3:** 1013–1019

Camasses A, Bogdanova A, Shevchenko A, Zachariae W (2003) The CCT chaperonin promotes activation of the anaphase-promoting complex through the generation of functional Cdc20. *Mol Cell* **12:** 87–100

Capron A, krész L, Genschik P (2003) First glance at the plant APC/C, a highly conserved ubiquitin-protein ligase. *Trends Plant Sci* **8:** 83–89

Chen H, Zou Y, Shang Y, Lin H, Wang Y, Cai R, Tang X, Zhou J-M (2008) Firefly luciferase complementation imaging assay for protein–protein interactions in plants. *Plant Physiol* **146:** 368–376

Churchman ML, Brown ML, Kato N, Kirik V, Hülskamp M, Inzé D, De Veylder L, Walker JD, Zheng Z, Oppenheimer DG, Gwin T, Churchman J, Larkin JC (2006) SIAMESE, a plant-specific cell cycle regulator, controls endoreplication onset in *Arabidopsis thaliana*. *Plant Cell* **18:** 3145–3157

Cui J, Li P, Li G, Xu F, Zhao C, Li Y, Yang Z, Wang G, Yu Q, Li Y, Shi T (2008) AtPID: *Arabidopsis thaliana* protein interactome database—an integrative platform for plant systems biology. *Nucleic Acids Res* **36:** D999–D1008

De Bodt S, Proost S, Vandepoele K, Rouzé P, Van de Peer Y (2009) Predicting protein–protein interactions in *Arabidopsis thaliana* through integration of orthology, gene ontology and co-expression. *BMC Genomics* **10:** 288

De Veylder L, Segers G, Glab N, Van Montagu M, Inzé D (1997) Identification of proteins interacting with the *Arabidopsis* Cdc2aAt protein. *J Exp Bot* **48:** 2113–2114

De Veylder L, Beeckman T, Inzé D (2007) The ins and outs of the plant cell cycle. *Nat Rev Mol Cell Biol* **8:** 655–665

Devault A, Martinez A-M, Fesquet D, Labbé J-C, Morin N, Tassan J-P, Nigg EA, Cavadore J-C, Dorée M (1995) MAT1 ('*ménage à trois*') a new RING finger protein subunit stabilizing cyclin H-cdk7 complexes in starfish and *Xenopus* CAK. *EMBO J* **14:** 5027–5036

Erhardt M, Stoppin-Mellet V, Campagne S, Canaday J, Mutterer J, Fabian T, Sauter M, Muller T, Peter C, Lambert A-M, Schmit A-C (2002) *J Cell Sci* **115:** 2423–2431

Forment J, Naranjo MÁ, Roldán M, Serrano R, Vicente O (2002) Expression of *Arabidopsis* SR-like splicing proteins confers salt tolerance to yeast and transgenic plants. *Plant J* **30:** 511–519

Gunsalus KC, Ge H, Schetter AJ, Goldberg DS, Han J DJ, Hao T, Berriz GF, Bertin N, Huang J, Chuang L-S, Li N, Mani R, Hyman AA, Sönnichsen B, Echeverri CJ, Roth FP, Vidal M, Piano F (2005) Predictive models of molecular machines involved in *Caenorhabditis elegans* early embryogenesis. *Nature* **436:** 861–865

Geisler-Lee J, O'Toole N, Ammar R, Provart NJ, Millar AH, Geisler M (2007) A predicted interactome for *Arabidopsis*. *Plant Physiol* **145:** 317–329

Hase Y, Trung KH, Matsunaga T, Tanaka A (2006) A mutation in the *uvi4* gene promotes progression of endo-reduplication and confers increased tolerance towards ultraviolet B light. *Plant J* **46:** 317–326

Hayes MJ, Kimata Y, Wattam SL, Lindon C, Mao G, Yamano H, Fry AM (2006) Early mitotic degradation of Nek2A depends on Cdc20-independent interaction with the APC/C. *Nat Cell Biol* **8:** 607–614

Inzé D, De Veylder L (2006) Cell cycle regulation in plant development. *Annu Rev Genet* **40:** 77–105

Ishida S, Huang E, Zuzan H, Spang R, Leone G, West M, Nevins JR (2001) Role for E2F in control of both DNA replication and mitotic functions as revealed from DNA microarray analysis. *Mol Cell Biol* **21:** 4684–4699

Jensen LJ, Jensen TS, de Lichtenberg U, Brunak S, Bork P (2006) Co-evolution of transcriptional and post-translational cell-cycle regulation. *Nature* **443:** 594–597

Karimi M, Depicker A, Hilson P (2007) Recombinational cloning with plant Gateway vectors. *Plant Physiol* **145:** 1144–1154

Kerrien S, Alam-Faruque Y, Aranda B, Bancarz I, Bridge A, Derow C, Dimmer E, Feuermann M, Friedrichsen A, Huntley R, Kohler C, Khadake J, Leroy C, Liban A, Lieftink C, Montecchi-Palazzi L, Orchard S, Risse J, Robbe K, Roechert B *et al* (2007) IntAct—open source resource for molecular interaction data. *Nucleic Acids Res* **35:** D561–D565

Kimbara J, Endo TR, Nasuda S (2004) Characterization of the genes encoding for MAD2 homologues in wheat. *Chromosome Res* **12:** 703–714

Kono A, Umeda-Hara C, Lee J, Ito M, Uchimiya H, Umeda M (2003) *Arabidopsis* D-type cyclin CYCD4;1 is a novel cyclin partner of B2-type cyclin-dependent kinase. *Plant Physiol* **132:** 1315–1321

Lammens T, Li J, Leone G, De Veylder L (2009) Atypical E2Fs: new players in the E2F transcription factor family. *Trends Cell Biol* **19:** 111–118

Maere S, Heymans K, Kuiper M (2005) BiNGO: a cytoscape plugin to assess overrepresentation of gene ontology categories in biological networks. *Bioinformatics* **21:** 3448–3449

Magyar Z, De Veylder L, Atanassova A, Bakó L, Inzé D, Bögre L (2005) The role of the *Arabidopsis* E2FB transcription factor in regulating auxin-dependent cell division. *Plant Cell* **17:** 2527–2541

Marion J, Bach L, Bellec Y, Meyer C, Gissot L, Faure J-D (2008) Systematic analysis of protein subcellular localization and interaction using high-throughput transient transformation of *Arabidopsis* seedlings. *Plant J* **56:** 169–179

Mayer ML, Gygi SP, Aebersold R, Hieter P (2001) Identification of RFC(Ctf18p, Ctf8p, Dcc1p): an alternative RFC complex required for sister chromatid cohesion in *S. cerevisiae*. *Mol Cell* **7:** 959–970

Menges M, de Jager SM, Gruissem W, Murray JAH (2005) Global analysis of the core cell cycle regulators of *Arabidopsis* identifies novel genes, reveals multiple and highly specific profiles of expression and provides a coherent model for plant cell cycle control. *Plant J* **41:** 546–566

Menges M, Hennig L, Gruissem W, Murray JAH (2003) Genome-wide gene expression in an *Arabidopsis* cell suspension. *Plant Mol Biol* **53:** 423–442

Müller S, Smertenko A, Wagner V, Heinrich M, Hussey PJ, Hauser M-T (2004) The plant microtubule-associated protein AtMAP65-3/PLE is essential for cytokinetic phragmoplast function. *Curr Biol* **14:** 412–417

Neufeld TP, de la Cruz AFA, Johnston LA, Edgar BA (1998) Coordination of growth and cell division in the *Drosophila* wing. *Cell* **93:** 1183–1193

Peres A, Churchman ML, Hariharan S, Himanen K, Verkest A, Vandepoele K, Magyar Z, Hatzfeld Y, Van Der Schueren E, Beemster GTS, Frankard V, Larkin JC, Inzé D, De Veylder L (2007) Novel plant-specific cyclin-dependent kinase inhibitors induced by biotic and abiotic stresses. *J Biol Chem* **282:** 25588–25596

Rice P, Longden I, Bleasby A (2000) EMBOSS: the European Molecular Biology Open Software Suite. *Trends Genet* **16:** 276–277

Rohila JS, Chen M, Chen S, Chen J, Cerny R, Dardick C, Canlas P, Xu X, Gribskov M, Kanrar S, Zhu J-K, Ronald P, Fromm ME (2006) Protein–protein interactions of tandem affinity purification-tagged protein kinases in rice. *Plant J* **46:** 1–13

Seifert GJ (2004) Nucleotide sugar interconversions and cell wall biosynthesis: how to bring the inside to the outside. *Curr Opin Plant Biol* **7:** 277–284

Shannon P, Markiel A, Ozier O, Baliga NS, Wang JT, Ramage D, Amin N, Schwikowski B, Ideker T (2003) Cytoscape: a software environment for integrated models of biomolecular interaction networks. *Genome Res* **13:** 2498–2504

Shimotohno A, Umeda-Hara C, Bisova K, Uchimiya H, Umeda M (2004) The plant specific kinase CDKF;1 is involved in activating phosphorylation in cyclin-dependent kinase-activating kinases in *Arabidopsis*. *Plant Cell* **16:** 2954–2966

Shultz RW, Tatineni VM, Hanley-Bowdoin L, Thompson WF (2007) Genome-wide analysis of the core DNA replication machinery in the higher plants *Arabidopsis* and rice. *Plant Physiol* **144:** 1697–1714

Sterck L, Rombauts S, Vandepoele K, Rouzé P, Van de Peer Y (2007) How many genes are there in plants (and why are they there)? *Curr Opin Plant Biol* **10:** 199–203

Swarbreck D, Wilks C, Lamesch P, Berardini TZ, Garcia-Hernandez M, Foerster H, Li D, Meyer T, Muller R, Ploetz L, Radenbaugh A, Singh S, Swing V, Tissier C, Zhang P, Huala E (2008) The *Arabidopsis* Information Resource (TAIR): gene structure and function annotation. *Nucleic Acids Res* **36:** D1009–D1014

Thornton BR, Toczyski DP (2006) Precise destruction: an emerging picture of the APC. *Genes Dev* **20:** 3069–3078

Tsesmetzis N, Couchman M, Higgins J, Smith A, Doonan JH, Seifert GJ, Schmidt EE, Vastrik I, Birney E, Wu G, D'Eustachio P, Stein LD, Morris RJ, Bevan MW, Walsh SV (2008) *Arabidopsis* Reactome: a foundation knowledgebase for plant systems biology. *Plant Cell* **20:** 1426–1436

Van Leene J, Stals H, Eeckhout D, Persiau G, Van De Slijke E, Van Isterdael G, De Clercq A, Bonnet E, Laukens K, Remmerie N, Henderickx K, De Vijlder T, Abdelkrim A, Pharazyn A, Van Onckelen H, Inzé D, Witters E, De Jaeger G (2007) A tandem affinity purification-based technology platform to study the cell cycle interactome in *Arabidopsis thaliana*. *Mol Cell Proteomics* **6:** 1226–1238

Van Leene J, Witters E, Inzé D, De Jaeger G (2008) Boosting tandem affinity purification of plant protein complexes. *Trends Plant Sci* **13:** 517–520

Vandepoele K, Casneuf T, Van de Peer Y (2006) Identification of novel regulatory modules in dicotyledonous plants using expression data and comparative genomics. *Genome Biol* **7:** R103

Vandepoele K, Raes J, De Veylder L, Rouzé P, Rombauts S, Inzé D (2002) Genome-wide analysis of core cell cycle genes in *Arabidopsis*. *Plant Cell* **14:** 903–916

Vandepoele K, Vlieghe K, Florquin K, Hennig L, Beemster GTS, Gruissem W, Van de Peer Y, Inzé D, De Veylder L (2005) Genome-wide identification of potential plant E2F target genes. *Plant Physiol* **139:** 316–328

Vanstraelen M, Van Damme D, De Rycke R, Mylle E, Inzé D, Geelen D (2006) Cell cycle-dependent targeting of a kinesin at the plasma membrane demarcates the division site in plant cells. *Curr Biol* **16:** 308–314

Vastrik I, D'Eustachio P, Schmidt E, Gopinath G, Croft D, de Bono B, Gillespie M, Jassal B, Lewis S, Matthews L, Wu G, Birney E, Stein L (2007) Reactome: a knowledge base of biologic pathways and processes. *Genome Biol* **8:** R39 (Err. Genome Biol (2009) **10:** 402)

Vodermaier HC, Gieffers C, Maurer-Stroh S, Eisenhaber F, Peters J-M (2003) TPR subunits of the anaphase-promoting complex mediate binding to the activator protein CDH1. *Curr Biol* **13:** 1459–1468

Yu H, Braun P, Yildirim MA, Lemmens I, Venkatesan K, Sahalie J, Hirozane-Kishikawa T, Gebreab F, Li N, Simonis N, Hao T, Rual J F, Dricot A, Vazquez A, Murray RR, Simon C, Tardivo L, Tam S, Svrzikapa N, Fan C *et al* (2008) High-quality binary protein interaction map of the yeast interactome network. *Science* **322:** 104–110

Zhou Y, Niu H, Brandizzi F, Fowke LC, Wang H (2006) Molecular control of nuclear and subnuclear targeting of the plant CDK inhibitor ICK1 and ICK1-mediated nuclear transport of CDKA. *Plant Mol Biol* **62:** 261–278